

Molecular orientational motions in liquid crystals: A study by Raman and infrared band-shape analysis

M. P. Fontana* and B. Rosi*

Dipartimento di Fisica, Universita degli Studi di Parma, I-43100 Parma, Italy

N. Kirov and I. Dozov

Institute of Solid State Physics, 72 boulevard Lenin, Sofia 1113, Bulgaria

(Received 30 September 1985)

In this paper we report an extensive study of the relevant static and dynamic parameters connected to microscopic order and reorientational motion of single molecules in liquid-crystalline mesophases. In particular, we have studied the temperature dependence of the second- and fourth-order parameters $\langle P_2 \rangle$ and $\langle P_4 \rangle$, and of the spinning and tumbling diffusion coefficients D_{\parallel}^{\prime} and D_{\perp}^{\prime} in the nematic phase of several mesogens; some smectic phases were studied also. These results were obtained using a combined theoretical-experimental method newly developed by us, which allows the simultaneous determination of both static and dynamic parameters from the study of Raman and infrared band shapes by Fourier-transform analysis. The results are discussed in the framework of reorientational diffusion processes in anisotropic potentials. Implications on the nature of the nematic-isotropic phase transition are also given.

I. INTRODUCTION

Vibrational spectroscopy is a major tool for the study of vibrational and reorientational relaxations in molecular fluids.^{1,2} For complex molecules, band-shape analysis of infrared (ir) and Raman spectra can be quite useful because of its sensitivity to specific molecular groups or subunits in the molecule. The spectral band shape is connected to the Fourier transform of the time autocorrelation function of the induced dipole (ir) or the polarizability (Raman) fluctuations; in principle, both vibrational and rotational relaxations of the single molecules contribute concurrently to the bandwidth. For complex molecules the multiplicity of vibrational manifolds and anharmonicities, coupled with the relatively large moments of inertia, cause the rotational contribution to be small compared to the vibrational one. A simplifying assumption, which is expected to be reasonably accurate for internal molecular modes of high frequency (say $\omega > 500 \text{ cm}^{-1}$), consists of separating the vibrational and rotational relaxations, thus neglecting the effect of the eventual rotovibrational coupling on the molecular dynamics. In this case the correlation functions factor out into the separate vibrational and rotational components respectively.

Even within such an approximation, however, it is exceedingly difficult to obtain the rotational correlation functions from ir spectra. We have already mentioned the small size of the rotational contribution to the bandwidth relative to the vibrational one. Furthermore, ir absorption is connected to the fluctuations of a vector quantity (i.e., $l=1$, where l is the main spherical-harmonics index); in an isotropic molecular fluid, there is no way to obtain separately the two components of the product correlation function. Thus it is necessary to estimate the vibrational part from some other measurements (typically the temperature dependence of the ir bandwidth, or the Raman

spectrum of the same band, when measurable), coupled with some theoretical model for the vibrational relaxation itself. In practice, and particularly in temperature-dependence studies, these difficulties restrict the applicability of ir spectroscopy to simple molecular systems and to only semiquantitative determinations of the relevant parameters.

Raman spectroscopy, probing as it does the fluctuations of a tensor quantity ($l=2$), allows in principle the determination of the vibrational and rotational contributions since it yields two pieces of information, namely the so-called polarized (VV) and depolarized (VH) spectra for each vibrational mode. For complex molecules, however, the tensorial nature of the process makes the connection between vibrational modes of the molecule and molecular reorientational motion less direct and less easy to visualize. This difficulty instead is less severe in ir spectroscopy. Thus, although Raman spectroscopy is in principle quite general in its applicability, in practice if used by itself it may yield only semiquantitative information on rotational correlations and their temperature dependence.

Most difficulties could be overcome if *both* Raman and ir band-shape analysis could be performed on the same system. This may be the case of anisotropic fluids, such as for instance oriented liquid-crystalline phases, as we have shown in two previous papers, hereinafter denoted paper I and II, respectively.^{3,4} In the following paragraph we shall briefly summarize the fundamentals and relevant algebra of our method, which allows in principle the determination of the cylindrical symmetry orientational order parameters $\langle P_2 \rangle$ and $\langle P_4 \rangle$, i.e., the two lowest-order coefficients of the series expansion of the nematic angular distribution function $f(\beta)$,⁵ and the two major components of the rotational diffusion tensor; these, for the strongly anisotropic, quasicylindrical mesogen molecules, reduce to the reorientational microscopic diffusion

coefficients $D_{||}^r$ (molecular spinning about the main symmetry axis) and D_{\perp}^r (molecular tumbling perpendicularly to the main symmetry axis).

In papers I and II we endeavored to establish the experimental and theoretical methods and checked them against existing results. In this paper we report an extensive study of all the relevant static and dynamic parameters connected to microscopic order and reorientational motion in nematic phases. In particular, the temperature dependence of $\langle P_2 \rangle$, $D_{||}^r$, D_{\perp}^r , and also $\tau_{||}^r$ and τ_{\perp}^r (the corresponding relaxation times) was studied carefully in the nematic phase, in the neighborhood of the N - I (nematic-isotropic) phase transition and well within the smectic phase.

II. RAMAN AND ir CORRELATION FUNCTIONS

A. ir Absorption

Consider a well collimated linearly polarized beam of light incident on a nematic sample aligned along the z axis (see Fig. 1). If a given normal vibrational mode q_v is

ir active, light will be absorbed at frequency ω and the resulting spectral band shape will be given by⁶

$$A_i(\omega) = (2\pi/\hbar c V) g(\omega) [1 - \exp(-\hbar\omega/kT)] \times \int_{-\infty}^{\infty} C_{m_i}(t) \exp(-i\omega t) dt, \quad (1)$$

where $C_{m_i}(t)$ is the induced dipole correlation function, $i=z,x$ stands for the incident light polarization, $g(\omega)$ contains weakly frequency-dependent factors such as local-field correction, index of refraction, oscillator amplitude. As stated before, the time correlation function may be factored out into its reorientational and vibrational components. The vibrational part as well as $g(\omega)$ and the Bose-Einstein population term factor out when we take the ratio

$$a_z(t)/a_x(t) = \frac{\langle m_z^y(0)m_z(t) \rangle / \langle m_z^y(0)m_z(0) \rangle}{\langle m_x^y(0)m_x(t) \rangle / \langle m_x^y(0)m_x(0) \rangle}, \quad (2)$$

where $m_i^y(t) = (dm_i/dq^y)_{q^y=0}$, and

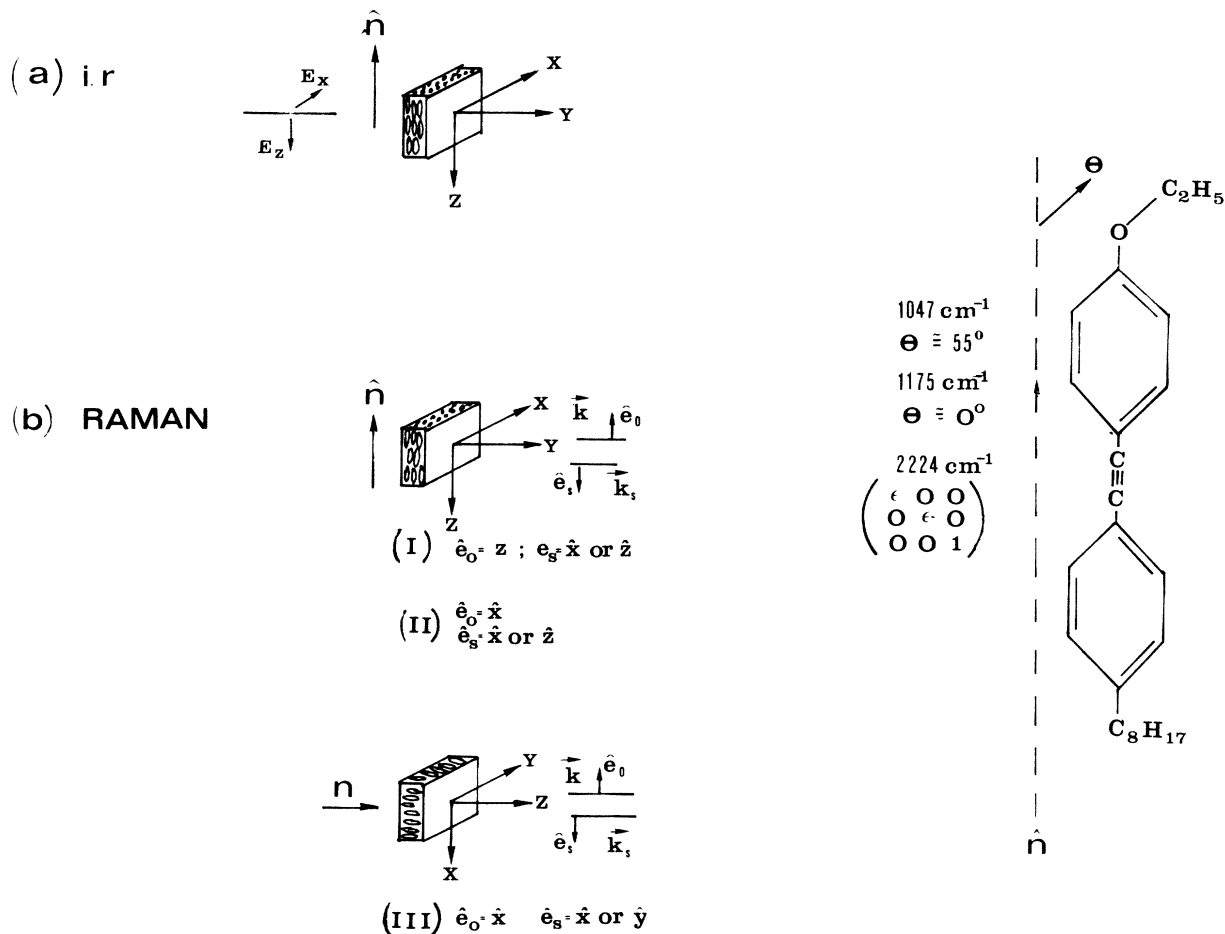


FIG. 1. Experimental geometries. (a) ir absorption; \hat{n} is the nematic director. Incident light propagates along Y . (b) Raman scattering; the experiment is performed in backscattering geometry and for homogeneous (I,II) and homeotropic configurations (III). In the figure we show also the characteristics of the ir and Raman vibrations we used which are relevant to molecular reorientations; θ is the angle between transition dipole moment (ir case) and molecular axis (perfect alignment is assumed). The Raman tensor is assumed uniaxial, i.e., $\epsilon \ll 1$. The molecule shown is OET.

$$a_i(t) = \frac{\int A_i(\omega) \exp(i\omega t) d\omega}{\int A_i(\omega) d\omega} \quad (3)$$

are the correlation coefficients, i.e., the normalized Fourier transform of the absorption band shape $A_i(\omega)$. The ratio $a_z(t)/a_x(t)$ thus yields directly the reorientational time correlation for those motions which modulate the molecular dipole moment induced by the vibrational mode q^ν .

Consider for instance the case of an induced dipole parallel to the molecular axis (Fig. 1). The spinning molecular motion is not expected to contribute appreciably to the band shape of the corresponding vibration. Thus spinning motion is not probed by such a band, which on the other hand is then suitable for studying the much slower tumbling motion. If the induced dipole makes an angle θ with the molecular axis (Fig. 1), spinning motion will dominate the reorientational broadening. Its contribution will be maximum for $\theta \cong 55^\circ$, the "magic angle" at which the $l=2$ Legendre polynomial $P_2(\cos\theta)=0$. Thus a judicious choice of vibrational modes will yield a specific sensitivity to either spinning or tumbling reorientations of the single molecules.

Given the relatively large mass of mesogen molecules [a typical molecular weight is, for instance, 284 for [N-(4-ethoxybenzylidene)-4'-(*n*-butyl)aniline (EBBA)], the inertial region, i.e., the time interval within which the molecule may be assumed to be essentially free before the intermolecular torques begin to act and randomize the

motion, is quite small (say about 0.1 psec). Therefore the time correlation function of reorientational fluctuations tends to be an exponential over most of the time domain probed by our experiment (see following paragraph). Under such circumstances the full application of memory-function formalism⁷ to obtain the correlation function from a dynamical model in order to fit the experimental data is not necessary; any Debye-like diffusion model will be adequate. In papers I and II we have chosen the small-step rotational jump diffusion model^{5,8} to describe the reorientational dynamics in the short-time limit ($tD' \ll 1$). Such a choice was somewhat arbitrary, and mainly dictated by the necessity of testing our method using a well known and tried dynamical model. However, it is possible to discriminate between several possible dynamical models by analyzing the behavior of the time correlation function in the inertial region. We have done so, and the results of our analysis will be published elsewhere.⁹ Here we shall mention only the main result, on the average angle for the jump: for spinning motion, it turns out to be approximately 25° ; for tumbling motion, we get approximately 5° . Thus it turns out that the small-step model is certainly adequate for the tumbling reorientations, and maybe less so for the spinning ones.

The kinematics of the coordinate transformations from the laboratory frame to the molecular frame, and the dynamical problem are best treated in the framework of an irreducible tensor formalism.¹⁰ In the short-time-limit approximation we obtain³

$$\frac{d}{dt} [a_z(t)/a_x(t)] = \frac{9\langle P_2 \rangle P_2(\cos\theta) D'_\perp + \langle P_2 \rangle [1 - P_2(\cos\theta)] [1 + 2P_2(\cos\theta)] (D'_\parallel - D'_\perp)}{[1 - 2\langle P_2 \rangle P_2(\cos\theta)] [1 + 2\langle P_2 \rangle P_2(\cos\theta)]}, \quad (4)$$

where the order parameter $\langle P_2 \rangle$ may be determined independently from the value of the dichroism of a strongly longitudinally polarized absorption band:

$$\langle P_2 \rangle = \frac{R - 1}{R + 2}, \quad (5)$$

where

$$R = \int A_z(\omega) d\omega / \int A_x(\omega) d\omega.$$

If the spectral band shape is well approximated by a single Lorentzian, the reorientational diffusion coefficients may be obtained directly from the difference in full widths at half height (FWHH) of the $A_x(\omega)$ and $A_z(\omega)$ bands, respectively. If δ_x and δ_z are the FWHH of the bands we have

$$\delta_x - \delta_z \cong \frac{\langle P_2 \rangle D'_\parallel}{\pi c} \quad (6a)$$

($\theta \cong 55^\circ$: "perpendicular" bands), and

$$\delta_x - \delta_z = \frac{D'_\perp}{\pi c} \frac{9\langle P_2 \rangle}{(1 - \langle P_2 \rangle)(1 + 2\langle P_2 \rangle)} \quad (6b)$$

($\theta = 0^\circ$: "parallel" bands).

Using bandwidth analysis of course simplifies the treatment of the data considerably; however, it is convenient to

use the Fourier technique first, not only because it yields the time dependence of the correlation functions, but also to identify the time interval in which such functions may be assumed to be exponential, and thus to gauge to what extent such approximation is correct.

B. Raman spectroscopy

Our typical scattering geometry is shown in Fig. 1. Incident light at frequency ω_0 , polarized along \mathbf{e}_0 , is back-scattered at frequency ω , with polarization analyzed along \mathbf{e}_s . The scattered spectral density is given by⁶

$$I_{ik}(\omega) = (I_{ik}^0 / 2\pi c^4) (\omega - \omega_0)^4 \times \int C_{ik}(t) \exp(-i\omega t) dt, \quad (7)$$

where $i, k = x, y, z$ and $C_{ik}(t)$ is the polarizability correlation function, which again we assume to factor into a vibrational and a reorientational part. Following the treatment of paper II, we construct the normalized Fourier transforms of I_{ik} , namely the coefficients $a_{ik}(t)$, which will be given by

$$a_{ik}(t) = \frac{\langle q^\nu(0) q^\nu(t) \rangle \langle \alpha_{ik}^\nu(0) \alpha_{ik}^\nu(t) \rangle}{\langle q^\nu(0) q^\nu(0) \rangle \langle \alpha_{ik}^\nu(0) \alpha_{ik}^\nu(0) \rangle}, \quad (8)$$

where $\alpha_{ik}^\nu = \partial \alpha_{ik} / \partial q^\nu |_{q^\nu=0}$ is the differential polarizability

tensor which contains all anisotropic contributions to the scattering due to vibrational mode q^ν . By taking spectra in the so-called polarized (for instance zz) and depolarized (zx) geometries, we construct the correlation coefficients $a_{zz}(t)$ and $a_{zx}(t)$ and then take the difference of their natural logarithms. In this process the vibrational relaxation drops out, and we are left with the time behavior of the reorientational correlation function. In as much as the Raman band can be approximated by a Lorentzian, we obtain a straight line, the slope of which yields directly the reorientational correlation time τ' .

If now we consider a strongly anisotropic vibration, whose differential polarizability tensor may be assumed to be uniaxial, the Raman band will be sensitive mainly to spinning or tumbling motions, depending on whether the transition involves light polarization perpendicular or parallel to the main molecular axis, respectively. In practice most uniaxial Raman vibrations in complex molecules are parallel, and therefore yield information on the tumbling correlation time τ'_1 .

In the framework of the short-time approximation, and small-step rotational diffusion model, in paper II we have calculated the tumbling relaxation times for three experimental geometries:⁴

$$\frac{d}{dt}[a_{zz}(t) - a_{xx}(t)] = \frac{8}{3} D_1' \left[\frac{7 - 2.5\langle P_2 \rangle - 4.5\langle P_4 \rangle}{7 - 10\langle P_2 \rangle + 3\langle P_4 \rangle} - \frac{7 + 5\langle P_2 \rangle - 12\langle P_4 \rangle}{7 + 20\langle P_2 \rangle + 8\langle P_4 \rangle} \right], \quad (9a)$$

$$\frac{d}{dt}[a_{zz}(t) - a_{zx}(t)] = D_1' \left[6 \frac{7 + 2.5\langle P_2 \rangle + 8\langle P_4 \rangle}{7 + 5\langle P_2 \rangle - 12\langle P_4 \rangle} - \frac{8}{3} \frac{7 + 5\langle P_2 \rangle - 12\langle P_4 \rangle}{7 + 20\langle P_2 \rangle + 8\langle P_4 \rangle} \right], \quad (9b)$$

$$\frac{d}{dt}[a_{xx}(t) - a_{xy}(t)] = \frac{70}{3} D_1' \frac{1 - \langle P_2 \rangle}{7 - 10\langle P_2 \rangle + 3\langle P_4 \rangle}. \quad (9c)$$

As is apparent from Eqs. (9), the tensor character of the fundamental quantity which is modulated by the reorientational motions causes a dependence of the relaxation times not only on the order parameter $\langle P_2 \rangle$, as was the case for ir absorption, but also on the higher-order parameter $\langle P_4 \rangle$, which may then be determined also.

As was the case for ir absorption, if the band shapes can be approximated to Lorentzians, the diffusion coefficients and the order parameters may be obtained directly from the FWHH δ_{ik} . In this case Eqs. (9) still apply, with the substitution of $\pi c(\delta_{ik} - \delta_{i'k'})$ in place of the appropriate first derivative of the correlation function.

III. EXPERIMENTAL TECHNIQUES

Infrared spectra were taken with a dual beam spectrophotometer. Spectral resolution for most runs was set at 1 cm^{-1} . Whenever possible, the spectral range about each line was investigated over about 5–10 times its FWHH.

Sample thickness was chosen to yield optimum absorbance, i.e., a transmission of 10–30%, and was approximately $10 \mu\text{m}$ for most samples. Each run was repeated five times and the reported results are averages over these five runs. The sample cells consisted of two flat KBr ir grade windows separated by calibrated teflon spacers; the cell thickness was checked interferometrically. Molecular alignment in the nematic phase was achieved by rubbing the windows, for homogeneous configuration. For most samples a maximum value of $\langle P_2 \rangle$ between 0.6 and 0.7 could be obtained. Sample temperature was controlled by a thermostat which circulated water inside a brass block which housed the sample cell. Temperature stability was better than 0.03 K. Temperature uniformity throughout the sample was worse; the sample dimensions were $14 \times 7 \text{ mm}^2$ and we estimated a temperature differential between the center and the periphery of the sample of about 0.3 K. For this reason we have not been able to probe the critical region, at least for $\epsilon < 10^{-3}$, where $\epsilon = (T_c - T)/T_c$ is the reduced temperature. It turns out that the problem of temperature inhomogeneity is not so severe as it may seem *a priori*. In fact, it should be much worse for ir spectra, where the beam size is about $10 \times 5 \text{ mm}^2$, than for Raman spectra, where the scattering section is less than $0.2 \times 0.1 \text{ mm}^2$. If inhomogeneity did induce significant systematic errors in the temperature dependence of the data, it should have very different effects on ir and Raman spectra. We have found this not to be the case, although as we shall see the absolute values of the same parameter (i.e., D_1') obtained using the two techniques are somewhat different.

Raman spectra were taken with a microprocessor driven and controlled spectrometric system; the computer also acted as data buffer.¹¹ Spectra were obtained mainly with the 4880-Å argon laser line, which was cylindrically focused onto the sample cell in a backscattering geometry (Fig. 1). Sample thickness was generally set at $50 \mu\text{m}$, a compromise between acceptable signal-to-noise ratio and minimization of polarization scrambling effects in the birefringent nematic phase.^{12,4}

Excitation power flux at the sample was always kept at a value of 100 W/cm^2 or less, in order to avoid sample damage or turbulence effects. In order to improve statistics in the rather stringent conditions of our experiment, each Raman band was iterated at least 20 times, yielding average integration times of 20 to 50 sec per channel. We used the standard VV (e.g., zz or xx) and VH (e.g., zx or xy) polarization geometries. The corresponding "polarized" and "depolarized" spectra were taken for the homogeneous and the homeotropic configurations, respectively (see Fig. 1). Homogeneous alignment was obtained by rubbing the cell windows, whereas the homeotropic configuration was achieved by treating the window surface with polysilane.

The mesogens studied were PMT [4-(*n*-pentyl)-4'-methoxytolane], HET [4-(*n*-heptyl)-4'-ethoxytolane], OET [4-(*n*-octyl)-4'-ethoxytolane], EBBA [N-(4-ethoxybenzylidene)-4'-(*n*-butyl)aniline], NPOOB [4-nitrophenyl-4'-(*n*-octyloxy)benzoate], and HOBDO [4-(*n*-hexyloxy)-4'-(*n*-decyloxy)benzoate]. The relevant transition temperatures for these compounds are as follows. For PMT, $C-N$ at

43.5°C and $N-I$ at 56.2°C; for HET, $C-N$ at 52.0°C and $N-I$ at 72.0°C; for OET, $C-N$ at 48.2°C and $N-I$ at 74.8°C; for EBBA, $C-N$ at 37.0°C and $N-I$ at 78.0°C; for NPOOB, $C-S_A$ at 51.2°C, S_A-N at 61.8°C, and $N-I$ at 68.7°C; for HOBDOP, $C-S_C$ at 62.5°C, S_C-S_A at 77.5°C, S_A-N at 83°C, and $N-I$ at 89°C.

The transition temperatures were determined spectroscopically and calorimetrically. For more details on experimental techniques, data handling, dynamical models, and calculations, we refer the reader to papers I and II.

IV. SPECTROSCOPY

The following ir modes were selected to determine D_{\parallel}^r and D_{\perp}^r : 1047 cm^{-1} (PMT, OET, HET), 1048 cm^{-1} (EBBA), 1175 cm^{-1} (OET, HET), 1178 cm^{-1} (PMT), 765 and 1743 cm^{-1} (NPOOB), and 1730 cm^{-1} (HOBDOP). The modes at 1047 and 1048 cm^{-1} are assigned to oxygen-alkyl tail stretching; they are weakly polarized (dichroic ratio $R = 1.8$). The band at 1743 cm^{-1} (and 1730 cm^{-1}) is attributed to carbonyl group stretching; for this band, $R = 0.9$. The transition dipole moment of these vibrational modes is directed to a good approximation along the magic angle, i.e., about 55° away from the long molecular axis. At such an angle the Legendre polynomial $P_2(\cos\theta) = 0$, and the modulation effect of the spinning motion on the transition dipole moment is maximum. These bands then will be most sensitive to the spinning diffusion coefficient D_{\parallel}^r ; since in general, and specifically in our experiments, $D_{\parallel}^r \gg D_{\perp}^r$, these bands will probe only D_{\parallel}^r . The transition dipole moment of the modes at 1175 and 1178 cm^{-1} (benzene ring in plane deformation) is essentially parallel to the molecular director ($R = 6$). Thus in this case the band shape will not be sensitive to the spinning motion, and it will be possible to determine the contribution to the band shape due to the tumbling reorientational motion, and thus the coefficient D_{\perp}^r .

In the case of ir spectra, the order parameter $\langle P_2 \rangle$ was determined independently using Eq. (5). For OET, HET, and PMT we used the integral intensity of the bands at 1175 and 1178 cm^{-1} , respectively. Since EBBA, HOBDOP, and NPOOB do not feature such strongly polarized Lorentzian longitudinal bands, for these mesogens we had to use the peak intensity of the lines corresponding to benzene ring stretching at 1495 cm^{-1} (NPOOB), 1605 cm^{-1} (EBBA), and 1518 cm^{-1} (HOBDOP).

Raman spectra were taken only for the tolane derivatives PMT, HET, and OET; for the other mesogens no suitable lines were available. We studied the band at 2224 cm^{-1} , corresponding to $C \equiv C$ stretching. The differential polarizability tensor of this line is expected to be highly anisotropic; thus a uniaxial tensor form may be used in the calculations.⁴ We have verified that this is indeed the case by determining the tensor elements experimentally, using the method introduced by Jen *et al.*¹² Thus we determined precisely the degree of depolarization $\rho = I_{VH}/I_{VV}$ of the 2224- cm^{-1} line in three scattering geometries in the nematic phase of PMT at 48°C. If the differential polarizability tensor diagonal elements are denoted by a , b , and c , we have

$$a = -0.02, \quad b = 0.065, \quad c \simeq 1.$$

The 2224- cm^{-1} Raman line is thus a good probe of tumbling molecular fluctuations. So far we have not been able to identify a Raman line which could be used to study the spinning molecular motions. Although in principle our method may be applied to Raman lines associated with nonuniaxial tensors, we have not been able to find lines of sufficient intensity and spectral quality, at least in the samples studied so far. Thus in this paper we are able to discuss only results on the tumbling diffusion coefficient D_{\perp}^r and correlation time τ_{\perp}^r , as far as Raman spectroscopy is concerned.

V. TEMPERATURE DEPENDENCE OF THE ORIENTATIONAL ORDER PARAMETERS $\langle P_2 \rangle$, $\langle P_4 \rangle$

In the case of the tolane derivatives, it was possible to determine $\langle P_2 \rangle$ from both ir and Raman spectra; the results could be compared, and this yields a test of the accuracy of the determination. In Fig. 2 we report the results on the temperature dependence of $\langle P_2 \rangle$ in the nematic phase of OET, obtained by studying the ir dichroism of the 1175- cm^{-1} band and using Eq. (5). In Fig. 2 we also show the behavior of both $\langle P_2 \rangle$ and $\langle P_4 \rangle$ as determined by Raman scattering; in this case the order parameters were obtained both using our method, i.e., by solving the system of equations (9) and by using the method of Jen *et al.*¹² As can be seen from the data, the two methods yield very similar results, well within the accuracy of our determinations; the small, systematic difference may be due to the different weight that local-field corrections have in the two methods. In any case the temperature dependence of the order parameters is unaffected, at least within the present experimental error. The agreement of ir and Raman data is also satisfactory; there appears to

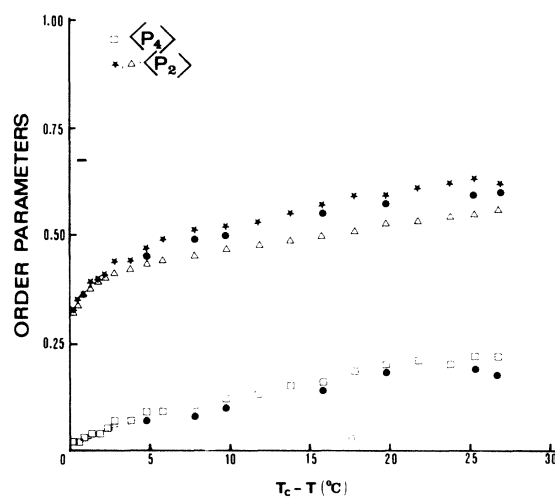


FIG. 2. Temperature dependence of the orientational order parameters: $\langle P_4 \rangle$ (\square) and $\langle P_2 \rangle$. $\langle P_2 \rangle$ was determined using the 1175- cm^{-1} ir band (\triangle) and the 2224- cm^{-1} Raman band ($*$). Solid circles denote the values of $\langle P_2 \rangle$ and $\langle P_4 \rangle$ we obtained using the method of Jen *et al.* (Ref. 13); they are not represented in the interval 0–5°C for $T_c - T$, as they are in complete agreement with our results.

be, however, a systematic discrepancy between the data. This is due to the fact that the ir data are not corrected for the index of refraction and its variation with temperature. No data are available in the literature on the index of refraction in the ir spectral range, and therefore we cannot attempt the correction. It is estimated that this may cause a systematic decrease of the measured value of $\langle P_2 \rangle$ of about 10%.¹³ Thus, although the ir data are more precise than the Raman data, the latter ones are more accurate, since their calculation by our method is independent of factors such as the index of refraction. Within the limits of our experimental accuracy, our data for $\langle P_2 \rangle$ and for $\langle P_4 \rangle$ agree with the data obtained by other methods on other nematic phases.¹⁴ In particular we wish to point out that, although our values for $\langle P_4 \rangle$ are systematically lower than theoretical predictions,¹⁵ they have the proper temperature behavior and are positive throughout the nematic phase; for our toluene derivatives then the majority of molecules have their axis within about 30° (corresponding to the first zero in the fourth-rank Legendre polynomial) of the nematic axis throughout the phase.⁵

VI. THE REORIENTATIONAL RELAXATION TIMES

In Fig. 3 we show a typical reorientational correlation function, obtained from the band-shape analysis of the Raman line at 2224 cm^{-1} in HET (nematic phase, $T = 63^\circ\text{C}$). The function is nearly exponential in the time domain $0.2 < t < 2$ psec. Our experimental resolution (2-cm^{-1} band-pass in the Raman case) did not allow us to probe longer times. Assuming that the correlation function is truly exponential, the Green-Kubo correlation time

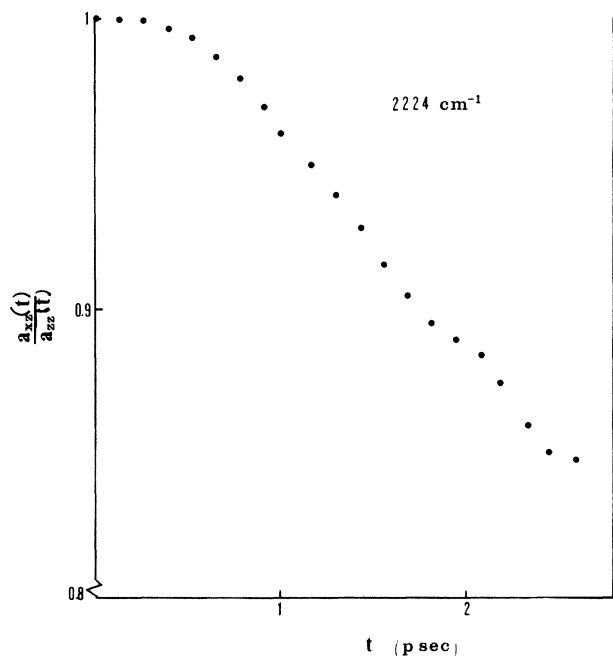


FIG. 3. Typical reorientational correlation function obtained from the 2224-cm^{-1} Raman band for HET at 63°C in the nematic phase.

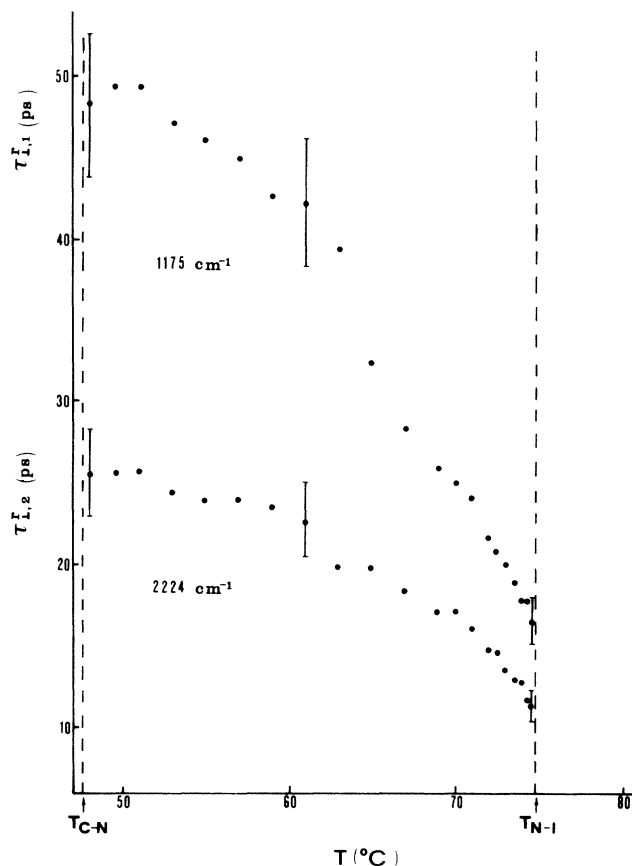


FIG. 4. Temperature dependence of $\tau_{I,1}^{\text{ir}}$ and $\tau_{I,2}^{\text{Raman}}$ in the nematic phase of OET. Tumbling diffusion is seen to behave as a normal, viscosity related thermally activated process.

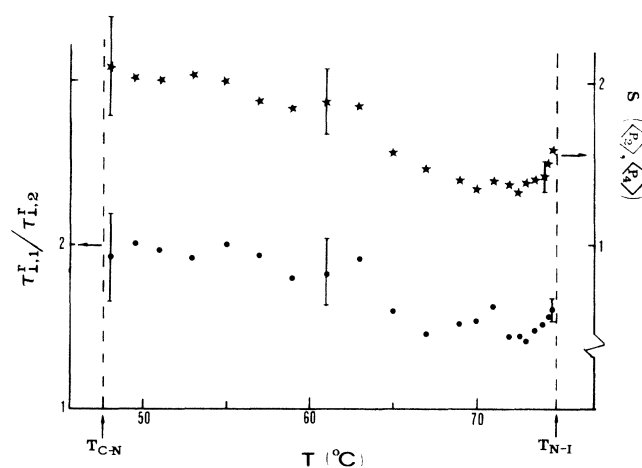


FIG. 5. Temperature dependence of the ratio $\tau_{I,1}^{\text{ir}}/\tau_{I,2}^{\text{Raman}}$ in the nematic phase of OET (lower points, ●); the upper points (*) refer to the "theoretical" behavior, as obtained by using the experimental values of $\langle P_2 \rangle$ and $\langle P_4 \rangle$ in the $\langle P_2 \rangle$ - and $\langle P_4 \rangle$ -dependent quantities in Eq. (9a) and corresponding equation for the ir case (Ref. 3), and constructing their ratio $S(\langle P_2 \rangle, \langle P_4 \rangle)$. Note the translation of ordinate axis.

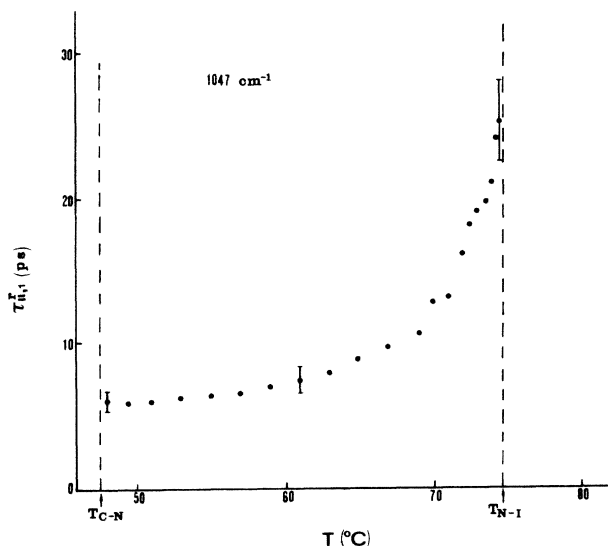


FIG. 6. Temperature dependence of the spinning relaxation time $\tau_{||,1}^r$ obtained for the nematic phase of OET using the 1047-cm^{-1} ir band.

(i.e., the time integral of the correlation function) coincides with the decay time τ^r of the correlation function. Within the limits of the exponential approximation, our data will yield directly the reorientational relaxation times $\tau_{||}^r$ and τ_{\perp}^r depending on the spectral line. In this sense the relaxation times give more fundamental information than the diffusion coefficients, whose value depends on the dynamical model chosen to solve the rotational diffusion equation. Furthermore, for the time being only for τ_{\perp}^r , we can obtain both $\tau_{\perp,1}^r$ (ir absorption) and $\tau_{\perp,2}^r$ (Raman

scattering); the temperature behavior of their ratio may be studied and information obtained on which type of reorientational model is more appropriate for the nematic phase.^{1,16}

In Fig. 4 we show the temperature dependence of $\tau_{\perp,1}^r$ and $\tau_{\perp,2}^r$ in the nematic phase of OET. τ_{\perp}^r decreases with increasing temperature as expected, following a roughly exponential law, yielding a typical Arrhenius activation energy of about 30 kcal/mol, which has the correct order of magnitude for these systems.¹⁷ Since there are no viscosity determinations for tolane derivatives, we could not test directly the linear dependence of τ_{\perp}^r on η/T (where η is an average shear viscosity), expected for any Debye-like diffusion model. However, using the published viscosity data for MBBA,¹⁸ whose nematic phase range is similar to that of OET, we indeed find that the expected Nernst-Einstein behavior of τ_{\perp}^r on η/T is followed.

In Fig. 5 we show a plot of the ratio $\tau_{\perp,1}^r/\tau_{\perp,2}^r$ versus temperature. The ratio remains essentially constant, at a typical value of approximately 2, throughout most of the nematic range. We note, however, a reasonably pronounced dip at about 60°C , and the hint of an increase close to T_{N-I} . For any Debye-like model of rotational diffusion in an isotropic fluid, $\tau^{(l=1)}/\tau^{(l=2)}=3$.^{1,16} The ratio decreases and tends to unity when the reorientational dynamics acquires more solidlike features (jump diffusion models), or when the reorientational events decrease in frequency but involve large rotation angles (strong collision models).

In our case, the small-step rotational diffusion model is expected to yield a good approximation for molecular tumbling motions. Thus the low values of the ratio must be connected to the anisotropy of the fluid, i.e., to the

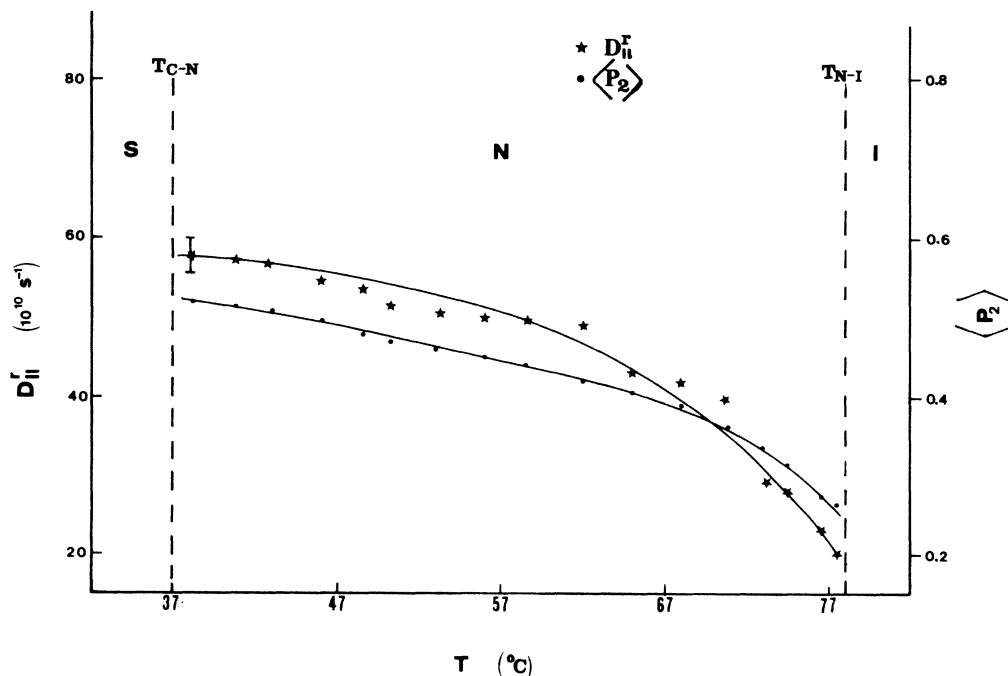


FIG. 7. Temperature dependence of the spinning diffusion coefficient $D_{||,1}^r$ and $\langle P_2 \rangle$ for the nematic phase of EBBA (\bullet , $\langle P_2 \rangle$; \star , $D_{||,1}^r$; 1048-cm^{-1} ir band).

nonzero values of the static order parameters. This is actually predicted by our Eqs. (9). In fact, if we plot the $\langle P_2 \rangle$ - and $\langle P_4 \rangle$ -dependent quantities in the appropriate ir and Raman equations, using the experimental values of $\langle P_2 \rangle$ and $\langle P_4 \rangle$, the resulting points are hardly distinguishable from the directly obtained experimental ones (Fig. 5). This result confirms the correctness of our choice of dynamical model; furthermore, it provides what we feel is the first direct experimental evidence on the effect of anisotropy on the behavior of a rotational correlation time in a fluid.

Totally different and quite startling is the temperature behavior of $\tau_{||,1}^r$, which, so far, we have been able to determine with the ir spectroscopy only. In Fig. 6 we show $\tau_{||,1}^r$ for the case of OET in the nematic phase. The spinning relaxation time $\tau_{||,1}^r$ increases substantially with temperature, particularly as T_{N-I} is approached. This slowing down of single molecule spinning fluctuations seems to be quite general; for instance, in Figs. 7 and 8 we show the results obtained for two other mesogens, namely EBBA and NPOOB. In the figures we have reported the calculated spinning diffusion coefficient $D_{||}^r$ instead of the relaxation time, to show more clearly the result that diffusion slows down as the orientational order decreases (the $\langle P_2 \rangle$ values as determined by us are also shown in the figures). Similar results have also been obtained for PMT, HET, and HOBDOP. From Fig. 8 it is apparent that $D_{||}^r$ is not very sensitive to the S_A -N transition. This is confirmed by our results for HOBDOP: as $\langle P_2 \rangle$ varies from 0.8 at the beginning of the S_A phase to 0.35 at the N -I transition, $\tau_{||,1}^r$ varies from 3.6 to 26 psec, without appreciable discontinuities at the phase transitions, at least on the coarse temperature scale of the measurements. These results are reasonable since $D_{||}^r$ measures single-particle rotational time correlations, and therefore should be insensitive to changes in the long-range order which leave the local molecular ordering unchanged.

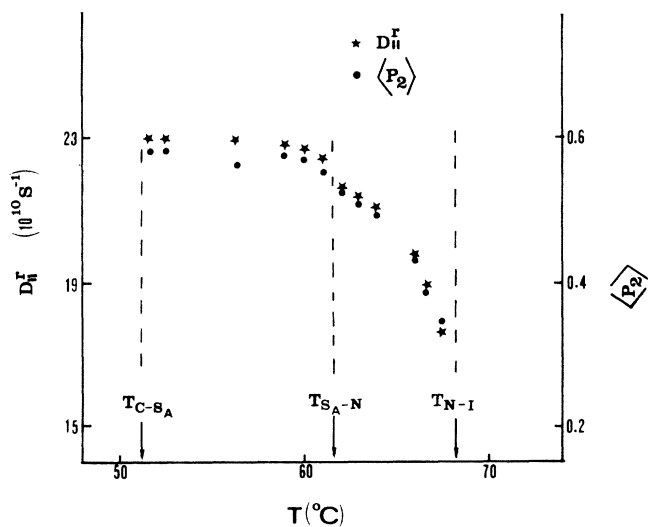


FIG. 8. Same as Fig. 7, for the S_A and nematic phases of NPOOB.

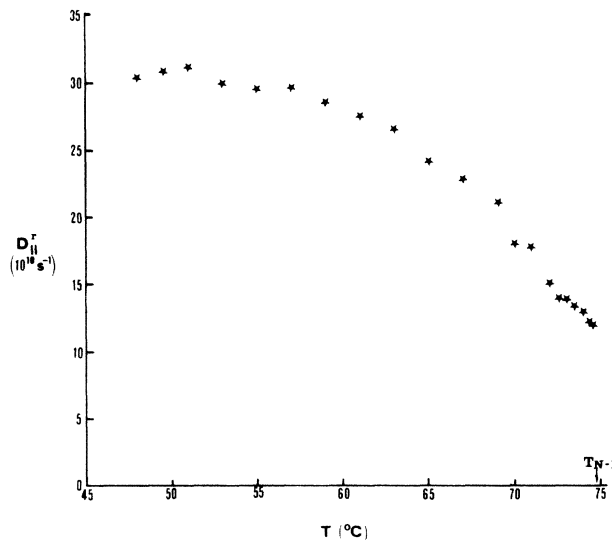


FIG. 9. Temperature dependence of the spinning diffusion coefficient $D_{||}^r$ in the nematic phase of OET (1047-cm^{-1} ir band).

In Figs. 9 and 10 we show the temperature dependence of the spinning and tumbling diffusion coefficients of OET in the nematic phase. The data show very graphically that the approach to isotropy takes place through a substantial pretransitional slowing down of the “longitudinal” component of the diffusion tensor. Such slowing down appears to take place over the whole mesophase region. At T_{N-I} , $D_{||}^r$ and D_{\perp}^r still differ by a factor of 5. Since D_{\perp}^r does not show any appreciable discontinuity at T_{N-I} , the question arises whether the difference in value between $D_{||}^r$ and D_{\perp}^r continues into the isotropic phase, and, if so, up to what temperature. Since so far we have not been able to determine $D_{||}^r$ directly in the isotropic phase, we cannot at this time provide an answer to this question.

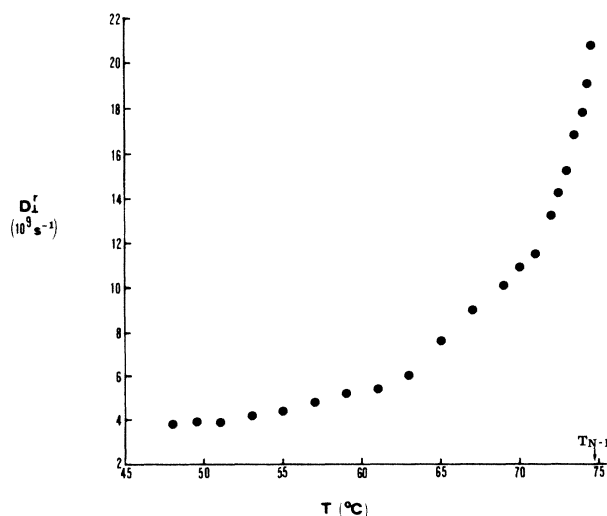


FIG. 10. Same as Fig. 9, for D_{\perp}^r (tumbling), from the 1175-cm^{-1} ir band.

VII. CONCLUSIVE REMARKS

The temperature dependence of the spinning relaxation time, perhaps the main result reported in this paper, requires some further analysis. Essentially two points of view may be adopted: the slowing down of spinning fluctuations with increasing temperature is due to the peculiarities of rotational diffusion in a strongly anisotropic fluid; alternatively or concurrently, the slowing down is "critical." Our calculations, which are based on a specific dynamical model, do yield the result that τ_{\parallel}^r should increase as the static order parameter $\langle P_2 \rangle$ decreases. Furthermore, our result agrees with a more general calculation of relaxation times in the presence of an ordering potential (19). However, neither our calculations nor the theory of Ref. 19 succeed in explaining quantitatively the strong temperature variation of τ_{\parallel}^r in the nematic phase. We, for instance, predict that

$$\tau_{\parallel}^r \sim (D_{\parallel}^r \langle P_2 \rangle)^{-1}$$

for the ir case. Since $\langle P_2 \rangle$ varies by a factor of about 2 in the nematic phase, the observed variation of about a factor of 4 in τ_{\parallel}^r is unexplainable, even assuming a total temperature independence of D_{\parallel}^r . A possible explanation could involve a deviation from uniaxiality in the nematic potential, i.e., a deviation from the assumed cylindrical symmetry of the molecules. Such a deviation is in fact entirely reasonable, and we expect it to have its most profound influence just on the spinning motion. The simplest way of taking into account molecular biaxiality is to include it into the nematic potential. Preliminary calculations based upon the small-step rotational diffusion model with a biaxial potential do indicate the possibility of a stronger dependence of τ_{\parallel}^r on $\langle P_2 \rangle$; in particular, if a certain delicate balancing between the two contributions (long axis and short axis) occurs, we could have the result that $\tau_{\parallel}^r \sim \langle P_2 \rangle^{-2}$. At this time, however, it is difficult to obtain quantitative results, since we know nothing about the relative size of the biaxial contribution to the potential. Furthermore we feel that a "static" explanation of the slowing down, depending as it does on a delicate balancing of contributions, may not be appropriate as a general explanation of the slowing down, which we encountered in all the samples we studied so far.

Thus we turn to the hypothesis that the slowing down is a general property of the nematic phase and is critical in nature. Although most evidence on pretransitional phenomena, and more particularly on critical slowing down of fluctuations, concerns the isotropic phase,²⁰ some evidence on pretransitional effects in the nematic phase has been reported.²¹ However, no data on dynamical effects in the nematic phase exist in the literature, as far as we know. A typical, widely known effect is the narrowing of the bandwidth in quasielastic light scattering.²² For $T > T_{N-I}$, director fluctuations of nematic "swarms" are seen to slow down as $T \rightarrow T_{N-I}$, following a law of the type

$$1/\tau \sim (T - T_0)^{\gamma}, \quad (10)$$

where $\gamma \sim 1$, $T_{N-I} - T_0 \lesssim 1^\circ\text{C}$. In the nematic phase in-

stead, long-range orientational order keeps the director fluctuations "locked" and the quasielastic light scattering is essentially independent of temperature throughout the phase.²³ On a molecular level, this result is reflected on our data on tumbling diffusion, which appear to follow the dynamics of an ordinary, temperature-activated process. The strong slowing down of the spinning fluctuations, however, does suggest that molecular spinning goes critical as $T \rightarrow T_{N-I}$ in the nematic phase. We have verified this hypothesis by fitting our data on τ_{\parallel}^r with a law such as (10). A log-log plot of $1/\tau_{\parallel}^r$ versus the reduced temperature $(T_0 - T)/T_0$ did yield a straight line for $T \geq 65^\circ\text{C}$, i.e., for $T_{N-I} - T \lesssim 10^\circ\text{C}$. However, such plot was linear only for an unreasonable value of T_0 ($T_0 - T_{N-I} \sim 5^\circ\text{C}$), and furthermore it did not take into account the role of rotational viscosity and its temperature dependence.²⁰ In fact, in a recent paper Lin²⁴ has shown (for the isotropic phase) that

$$1/\tau^r \sim \nu^{-1}(T - T_0), \quad (11)$$

where ν is an average rotational viscosity coefficient. In our case, since there are no published data on the viscosity of our tolane derivatives, we have used in place of ν , the results on the tumbling diffusion coefficient D_{\perp}^r , which we have already seen to have the proper temperature behavior. Thus we plotted $1/\tau_{\parallel}^r D_{\perp}^r$ versus reduced temperature. The critical temperature T_0 was varied to minimize the confidence parameters in a linear regression fit to the data. We obtain the best fit with $T_0 = T_{N-I} + 0.3^\circ\text{C}$ and $\gamma = 1.02 \pm 0.03$.²⁵ It is important to note that the linearity of the plot extends over the whole nematic range, at least as far as our temperature resolution and errors in the τ_{\parallel}^r values allowed us to estimate. The value of T_0 is also reasonable.²¹ The exponent γ turns out to have the classical value; this would confirm the view that the $N-I$ transition is classical, i.e., describable in terms of a Landau-de Gennes theory.²⁰ We must note, however, that if indeed the temperature behavior we observe is critical, it would imply the existence of a second critical fluid at the $N-I$ transition, namely that connected with biaxial fluctuations. In fact the dynamics of the spinning motion is heavily dependent on deviations from cylindrical symmetry of the molecules. Perfectly smooth cylindrical molecules would have a totally inertial motion in the ordered nematic phase. Thus biaxiality may enter not only statically by changing the form of the nematic potential, but also dynamically by correlating the spinning motions over an increasing number of molecules as each slows down because of the decrease in $\langle P_2 \rangle$ as $T \rightarrow T_{N-I}$. If the static contribution to the slowing down turns out to be less relevant than the dynamical one, our data would furnish strong support to the view that the $N-I$ transition is tricritical,²⁶ or at least quasitricritical.²⁷

The precise nature of the $N-I$ transition is still one of the outstanding problems in the field of critical phenomena. Both classical²⁸ and tricritical²⁶ behavior have been claimed or disputed. One obvious test to assign the transition should be the determination of β , the critical exponent connected with the behavior of the order parameter $\langle P_2 \rangle$ with temperature. Classical theory predicts $\beta = 0.5$, whereas for a tricritical point $\beta = 0.25$. The

determination of β , however, has proven to be particularly difficult and fraught with ambiguities, due mainly to the fact that the N - I transition is weakly first order. This implies that in the critical plot of $\langle P_2 \rangle$ versus T , three parameters come into play: the exponent β ; the "superheating" critical temperature T_0 ; and the extrapolated value of $\langle P_2 \rangle$ at T_0 , $\langle P_2 \rangle_0$. Clearly a log-log plot in which three parameters may be varied to yield a straight line is likely to lead to a wide range of possible choices of parameter values.

An analysis of many results on $\langle P_2 \rangle$ in the literature²⁹ shows that a value of $\beta=0.2$ would yield a satisfactory fit. More recent determinations³⁰ also would favor a low value for β , within the limits of ambiguity we have described. Since our method allows us to determine simultaneously the static order parameter $\langle P_2 \rangle$ and the dynamical parameter τ_{\parallel}^2 , we are able to decrease considerably the arbitrariness in a fit such as

$$\langle P_2 \rangle - \langle P_2 \rangle_0 \sim (T_0 - T)^\beta. \quad (12)$$

In fact, we may obtain a value for T_0 independently from the fit (11) of the temperature behavior of τ_{\parallel}^2 , then use it to fit Eq. (12). The number of free parameters is thus reduced to two, and this obviously should yield more definite results for β .

In Fig. 11 we show the critical plots and fits to Eq. (12) for the cases of OET [Fig. 11(a)] and EBBA [Fig. 11(b)]. For OET $T_0 = T_{N-I} + 0.3^\circ\text{C}$, and for EBBA $T_0 = T_{N-I} + 1^\circ\text{C}$. Keeping T_0 fixed at these values, we used a linear regression routine to fit the data; minimization of the statistical confidence parameters yielded the values

$$\langle P_2 \rangle_0 = 0.14, \quad \beta = 0.25 \quad \text{for OET};$$

$$\langle P_2 \rangle_0 = 0.1, \quad \beta = 0.3 \quad \text{for EBBA}.$$

Although these data would seem to confirm unequivocally the tricritical nature of the N - I transition, they are not of sufficiently high quality yet to allow a definitive statement. In particular, due to our relatively poor temperature resolution and consequent lack of experimental points for $T \sim T_{N-I}$, the precise assessment of the $\langle P_2 \rangle_0$ value was difficult, and the minimum of the confidence parameters in the fit is shallow. Thus our data (which are more precise for OET than for EBBA) only allow us to bracket

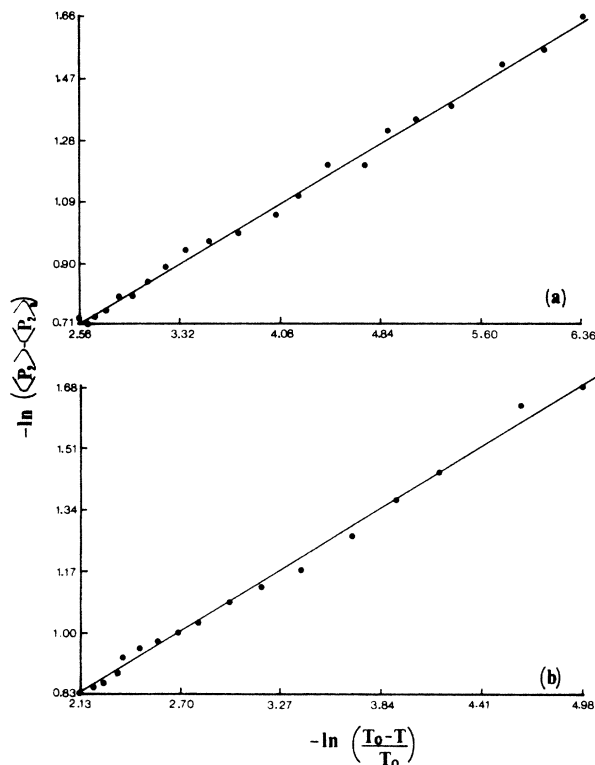


FIG. 11. (a) Critical plot of $\langle P_2 \rangle - \langle P_2 \rangle_0$ versus reduced temperature for OET: the solid line is the fit using Eq. (12). See main text for details. (b) Same as (a), for the case of EBBA.

β : $0.2 \lesssim \beta \lesssim 0.3$ (OET); $\beta \lesssim 0.35$ (EBBA). Our data are sufficiently unambiguous to exclude, at any rate, the result $\beta = 0.5$.

With improved temperature resolution, our method should yield a specific and clear answer to the problem of the value of β , since then the critical fit would have only β as a free parameter. We are presently working on this problem. Independently of what the final result may be, our work does show the importance of spinning fluctuations and of the interplay between the static and dynamic contributions of molecular biaxiality in determining the dynamics of the nematic phase and the nature of the N - I transition point.

*Also at Unità di Parma, Gruppo Nazionale di Struttura della Materia, Consiglio Nazionale delle Ricerche, I-43100 Parma, Italy and Unità di Parma, Centro Interuniversitario di Struttura della Materia, Ministero della Pubblica Istruzione, I-43100 Parma, Italy.

¹J. H. R. Clarke, in *Advances in IR and Raman Spectroscopy*, edited by R. J. H. Clark and R. E. Hester (Heyden, London, 1977), Vol. 4, p. 109.

²W. Rothschild, *Dynamics of Molecular Liquids* (Wiley, New York, 1984).

³I. Dozov, N. Korov, and M. P. Fontana, *J. Chem. Phys.* **81**, 2585 (1984).

⁴N. Kirov, I. Dozov, and M. P. Fontana, *J. Chem. Phys.* **83**, 5267 (1985).

⁵See, for instance, C. Zannoni, in *Nuclear Magnetic Resonance of Liquid Crystals*, edited by J. W. Emsley (Reidel, Dordrecht, 1985), p. 1.

⁶R. T. Bailey, in *Molecular Spectroscopy*, Chemical Society Specialist Periodical Report, edited by J. R. Durig (American Chemical Society, New York, 1974), Vol. 2, p. 173.

⁷See, for instance, M. Evans, in *Advances in Chemical Physics*, edited by I. Prigogine and S. A. Rice (Wiley, New York, 1980), Vol. 44, p. 255.

⁸Some relevant references on rotational diffusion are C. F. Pol-

- naczek, G. F. Bruno, and J. H. Freed, *J. Chem. Phys.* **58**, 3185 (1973); G. R. Luckhurst, M. Setaka, and C. Zannoni, *Mol. Phys.* **28**, 49 (1974); P. L. Nordio and P. Busolin, *J. Chem. Phys.* **55**, 5485 (1971); P. L. Nordio, G. Rigatti, and U. Segre, *Mol. Phys.* **25**, 129 (1973); C. Zannoni, *Mol. Phys.* **38**, 1813 (1979); P. L. Nordio and U. Segre, in *Molecular Physics of Liquid Crystals*, edited by G. R. Luckhurst and G. W. Gray (Academic, New York, 1979), p. 411.
- ⁹M. P. Fontana, N. Kirov, and I. Dozov (unpublished).
- ¹⁰M. E. Rose, *Elementary Theory of Angular Momentum* (Wiley, New York, 1957).
- ¹¹D. Bianchi, F. Cavatorta, and G. Lenzi, *Comput. Enhanc. Spectrosc.* **1**, 222 (1983).
- ¹²S. Jen, N. A. Clark, and P. S. Pershan, *J. Chem. Phys.* **66**, 4635 (1977), and their earlier publications cited therein; see also the review by P. S. Pershan, in *The Molecular Physics of Liquid Crystals*, edited by G. R. Luckhurst and G. W. Gray (Academic, New York, 1979), p. 385; the scrambling effect has been also discussed by K. Mijano, *J. Chem. Phys.* **69**, 4807 (1978).
- ¹³A. Saupe and W. Maier, *Z. Naturforsch.* **16a**, 816 (1961); see also F. R. Fernandes and S. Venugopalan, *Mol. Cryst. Liq. Cryst.* **35**, 113 (1976).
- ¹⁴E. B. Priestley, *RCA Rev.* **35**, 144 (1974); P. Sheng and P. J. Wojtowicz, *Phys. Rev. A* **14**, 1883 (1976); see also E. B. Priestley and P. J. Wojtowicz, in *Introduction to Liquid Crystals*, edited by E. B. Priestley, P. J. Wojtowicz, and P. Sheng (Plenum, New York, 1974), Chaps. 1, 3, 4, and 6; some more measurements of $\langle P_2 \rangle$ and $\langle P_4 \rangle$ temperature dependence are M. Kohli, K. Otnes, R. Pynn, and T. Riste, *Z. Phys. B* **24**, 147 (1976); G. R. Luckhurst and R. N. Yeates, *J. Chem. Soc. Faraday Trans. II* **72**, 996 (1976); S. Kobinata, Y. Nakajima, H. Yoshida, and S. Maeda, *Mol. Cryst. Liq. Cryst.* **66**, 67 (1981); L. G. P. Dalmolen and W. H. de Jeu, *J. Chem. Phys.* **78**, 7353 (1983); S. N. Prasad and S. Venugopalan, *ibid.* **75**, 3033 (1981); L. G. P. Dalmolen, E. Egberts, and W. H. de Jeu, *J. Phys. (Paris)* **45**, 129 (1984); N. Kirov, I. Dozov, and I. Penchev, *J. Mol. Liq.* (to be published).
- ¹⁵W. Maier and A. Saupe, *Z. Naturforsch.* **15a**, 287 (1960).
- ¹⁶B. J. Berne and R. Pecora, *Dynamic Light Scattering* (Wiley, New York, 1976).
- ¹⁷F. J. Bartoli and T. A. Litovitz, *J. Chem. Phys.* **56**, 404 (1972), and the literature therein; see also N. Kirov and P. Simova, *Spectrochim. Acta* **29A**, 56 (1973); P. Simova and N. Kirov, *Adv. Mol. Relaxation Interaction Processes* **5**, 233 (1973).
- ¹⁸N. Knepe and F. Schneider, *Mol. Cryst. Liq. Cryst.* **65**, 23 (1981); B. C. Benicewicz, J. F. Johnson, and N. T. Shaw, *ibid.* **65**, 111 (1981); H. Knepe and F. Schneider, *ibid.* **97**, 219 (1983).
- ¹⁹P. Grigolini and S. Romani, *Chem. Phys. Lett.* **116**, 487 (1985).
- ²⁰For a review of basic work, see P. G. de Gennes, *The Physics of Liquid Crystals* (Oxford University, Oxford, 1974), Chaps. 2 and 5.
- ²¹See, for instance, M. Schadt, *J. Chem. Phys.* **67**, 210 (1977); E. M. Aver'yanov, *Fiz. Tverd. Tela (Leningrad)* **24**, 265 (1982) [*Sov. Phys.—Solid State* **24**, 149 (1982)]; K. V. S. Rao, J. S. Hwang, J. H. Freed, *Phys. Rev. Lett.* **37**, 595 (1976); Y. Poggi, P. Atten, and R. Aleonard, *Phys. Rev. A* **14**, 466 (1976).
- ²²T. W. Stinson III and J. D. Litster, *Phys. Rev. Lett.* **25**, 503 (1970).
- ²³I. Haller and J. D. Litster, *Mol. Cryst. Liq. Cryst.* **12**, 277 (1971).
- ²⁴Lin Lei, *Mol. Cryst. Liq. Cryst.* **112**, 233 (1984).
- ²⁵For more details, see a preliminary report on this work: M. P. Fontana, B. Rosi, N. Kirov, *Phys. Rev. Lett.* (to be published).
- ²⁶P. H. Keyes, *Phys. Lett.* **67A**, 132 (1978); P. H. Keyes and J. R. Shane, *Phys. Rev. Lett.* **42**, 722 (1979).
- ²⁷J. Thoen, H. Marynissen, and W. Van Dael, *Phys. Rev. A* **26**, 2886 (1982).
- ²⁸Lin Lei, *Phys. Rev. Lett.* **43**, 1604 (1979); C. Rosenblatt, *Phys. Rev. A* **25**, 1239 (1982); **27**, 1234 (1983).
- ²⁹I. Haller, *Prog. Solid State Chem.* **10**, 103 (1975).
- ³⁰See, for instance, A. Buka and W. H. de Jeu, *J. Phys. (Paris)* **43**, 361 (1982).